Vegetative growth, biomass allocation, and chlorophyll fluorescence of vanilla (Vanilla planifolia) as affected by light intensity and nitrogen supply

Marvin Vahl

m.vahl@hs-osnabrueck.de

Osnabrück University of Applied Sciences

Jannis Salzen

Osnabrück University of Applied Sciences

Antonia Jeismann

Osnabrück University of Applied Sciences

Finn Petersen

Osnabrück University of Applied Sciences

Andreas Ulbrich

Osnabrück University of Applied Sciences

Research Article

Keywords:

DOI: https://doi.org/

Additional Declarations: No competing interests reported.

Vegetative growth, biomass allocation, and chlorophyll fluorescence of vanilla (*Vanilla planifolia*) as affected by light intensity and nitrogen supply

Marvin Vahl* (m.vahl@hs-osnabrueck.de), Jannis von Salzen (jannis.vonsalzen@hs-osnabrueck.de), Antonia Jeismann (Antonia.j@web.de), Finn Petersen (finn.petersen@hs-osnabrueck.de), Andreas Ulbrich (a.ulbrich@hs-osnabrueck.de)

Osnabrück University of Applied Sciences, Faculty of Agricultural Sciences and Landscape Architecture, Am Krümpel 31, 49082 Osnabrück, Germany

*Corresponding Author:
Marvin Vahl
Faculty of Agricultural Sciences and Landscape Architecture
Osnabrück University of Applied Sciences
Am Krümpel 31, 49082 Osnabrück, Germany
Email: m.vahl@hs-osnabrueck.de
Phone: +49 541 969-5352

Keywords
Hydroponics, Fertilisation, Light, Nitrogen, Nutrients, Vanilla

Abstract

This study quantified the individual and interactive effects of photosynthetic photon flux (PPFD) density and nitrate-nitrogen supply on vegetative growth of *Vanilla planifolia (V. planifolia)* in a factorial experiment combining four PPFD levels (10-208 µmol m^{-2} s^{-1}) and six nitrogen concentrations (6.9-60.5 mg NO_3^--N L^{-1}) over 154 days. Light intensity was the dominant factor, affecting 16 of 20 parameters. Biomass gain saturated at 125 µmol m^{-2} s^{-1} (daily light integral ~5.4 mol m^{-2} d^{-1}), while specific leaf area halved, indicating structural acclimation. Non-photochemical quenching rose 20-fold without an increase in non-regulated dissipation, consistent with regulated photoprotection. Nitrogen optimised biomass

production efficiency at approximately 50-56 mg L^{-1}, and leaf nitrogen saturated near 2.1-2.2% dry mass. Light × nitrogen interactions were scarce (4 of 20 parameters), indicating that nitrogen demand was largely independent of light within the range tested. PSII fluorescence parameters responded exclusively to light; Y(NO) was unresponsive to both factors. The results provide the first PPFD and nitrogen dose-response data for *V. planifolia* and, as an outcome from this soilless system, support a target of 125 µmol m^{-2} s^{-1} PPFD for highest growth and 50-56 mg NO_3^--N L^{-1} for optimal nitrogen-use efficiency in vegetative cultivation.

Introduction

Vanilla planifolia (*V. planifolia)* is the main commercial source of natural vanilla, one of the most widely used flavourings in the food, cosmetic, and pharmaceutical industries [1]. Global production of raw vanilla averaged 7,139 tonnes per year over 2022-2024, with Madagascar, Indonesia, and Mexico accounting for the majority of output [2]. Despite sustained demand, production remains vulnerable to a combination of biological and economic constraints that act simultaneously on the same plantations. On the economic side, the vanilla market is characterised by extreme price volatility [3]: farmgate prices for green vanilla in the SAVA region of Madagascar collapsed from an average of around 36 € kg^{-1} in 2018 to around 2 € kg^{-1} in 2023, a decline of roughly 94% [4]. Foremost among the biological constraints is *Fusarium oxysporum* (*F. oxysporum*) f. sp. *radicis-vanillae*, the causal agent of root and stem rot, a major pathogen of vanilla worldwide that causes progressive necrosis of roots, ultimately leads to total plant collapse, and is therefore responsible for substantial yield losses [5,6]. In parallel, the exceptionally narrow genetic base of the cultivated crop, resulting from centuries of clonal propagation, renders cultivated lineages particularly susceptible to biotic and abiotic stresses, a vulnerability that climate change is expected to aggravate further [7,8]. Together, these pressures have stimulated interest in diversifying production methods, including pilot-scale greenhouse cultivation [9], intensified net-house cultivation with fertigation, and, more recently, first explorations of substrate-free hydroponic systems [1,10].

Optimising such controlled cultivation systems requires matching conditions to the physiological constraints of the species. As a crassulacean acid metabolism (CAM) orchid native to the shaded understorey of tropical forests, *V. planifolia* has a photosynthetic physiology adapted to low-light environments [11,12]. The species requires shade for adequate growth and suffers chronic photoinhibition at high irradiance [13]. Vegetative growth of *V. planifolia* has been shown to be highest at intermediate relative illumination (17-31%, corresponding to a maximum photosynthetic photon flux density (PPFD) of 369-577 µmol m^{-2} s^{-1}) and to be strongly inhibited at 67% relative illumination (1285 µmol m^{-2} s^{-1}) [13], while spectral light quality has been reported to influence leaf growth, chlorophyll content, and nocturnal CO_2 assimilation under photoselective shade netting [14]. Under a maximum PPFD of 200 µmol m^{-2} s^{-1}, the effective quantum yield of photosystem II (Y(II)) measured at 132 µmol m^{-2} s^{-1} declined from 0.7 in the morning to 0.55 in the afternoon, and non-photochemical quenching (NPQ) rose from 0.5 to 1.4 as CO_2 assimilation decreased over the day due to depletion of the malic acid pool [15]. Within the Orchidaceae, the well-studied CAM genus *Phalaenopsis* serves as a useful, though phylogenetically distant, physiological comparator, with several studies on this genus illustrating light-dependent growth and carbon-gain responses across the same PPFD range relevant to *V. planifolia*. Raising PPFD from 60 to 140 µmol m^{-2} s^{-1} during a 15-19-week vegetative phase of Phalaenopsis increased total dry mass by 21-30% across 14-19 genotypes, with root dry mass increasing by 41-55% [16]. At a daily light integral (DLI) of 5.6 mol m^{-2} d^{-1}, diel carbon gain was governed by the irradiance received during CAM phase III rather than the total DLI, and declined by 25% when phase-III irradiance was halved from 120 to 60 µmol m^{-2} s^{-1} [17]; and photosynthetic acclimation across 10-200 µmol m^{-2} s^{-1} PPFD has recently been confirmed in *Phalaenopsis* [18].

Within this low-light niche, light intensity and nitrogen supply are two environmental variables that directly govern vegetative biomass production, and their interplay is fundamental to plant carbon-nutrient

balance. Higher irradiance generally increases nitrogen demand by driving photosynthetic carbon fixation and creating a larger sink for amino acid and chlorophyll biosynthesis [19,20]; for shade-adapted CAM species, however, this coupling may be weakened because carbon fixation capacity is inherently constrained by both the low-light niche and CAM biochemistry [12]. Whereas the influence of light on *V. planifolia* growth has been at least partially characterised, its nitrogen requirements have not. In traditional agroforestry systems, which still account for the majority of global vanilla production [4], nutrition is provided implicitly through decomposing leaf litter, compost, host-tree root interactions, and mycorrhizal associations [21], while external mineral fertilisation is often absent or limited to coarse NPK applications [1,22]. The few available studies examined fertiliser type and dose effects on flowering and leaf nutrient status in field-grown vanilla but did not isolate nitrogen as a single variable, and used organic substrates in which mineralisation and buffering preclude precise control of nitrogen supply to the root zone [23–25]. In better-studied epiphytic orchids, by contrast, root-zone nitrogen concentration is a primary determinant of vegetative growth, with sufficiency ranges reported around 100 mg L^{-1} for *Dendrobium* [26] and 100-200 mg L^{-1} for *Phalaenopsis*, with diminishing or negative returns at higher concentrations [27,28].

Beyond identifying a growth optimum, precise nitrogen management is essential for plant health and environmental sustainability. Excess nitrogen can increase susceptibility to fungal pathogens [29], a particularly relevant concern given the threat of *F. oxysporum* in vanilla, and surplus nitrogen lost to the environment contributes to eutrophication and groundwater contamination [30]. Defining a sufficiency rather than a maximum-tolerance dose is therefore important not only agronomically but also for the long-term viability of intensified vanilla production.

Despite these considerations, quantitative dose-response data are lacking for *V. planifolia* with respect to both PPFD and nitrogen supply. Most existing light-response studies were conducted under shade cloth or natural canopy with uncontrolled or unreported PPFD and DLI, so that a PPFD dose-response

under defined spectral and photoperiod conditions has not been established [13–15]. The nitrogen dose that supports optimal vegetative growth has never been systematically determined, and the optimal nitrogen level under different PPFD conditions, i.e., the pairing of light-driven growth with nitrogen supply, remains uncharacterised. Given the economic importance of the crop and the challenges posed by *Fusarium* wilt, closing these gaps is a prerequisite for evidence-based fertilisation and lighting guidelines. Against this background, the objectives of this study were (i) to quantify the individual and interactive effects of PPFD and NO_3^--N supply on vegetative growth, biomass allocation, and leaf physiology of *V. planifolia* grown in a controlled environment; and (ii) to determine the nitrogen dose-response relationship for key growth and efficiency parameters across a range of PPFD levels and to estimate the optimal nitrogen concentration for maximising biomass production efficiency.

Materials and Methods

Plant material and pre-cultivation

The *V. planifolia* mother plants used for propagation of the cuttings in this study originated entirely from the commercial orchid nursery Röllke Orchideen GbR (Flößweg 11, 33758 Schloß Holte-Stukenbrock, Germany). The procurement was handled by botconsult GmbH (Heiligenberg, Germany) on behalf of Symrise AG (Holzminden, Germany). The supplier states that every *Vanilla* plant it distributes traces back to a virus-free meristem culture line that was established in 1985; this line has been propagated vegetatively and kept under controlled nursery conditions ever since, and no material of wild origin was incorporated. From 6 September 2021 onward, the mother plants were grown hydroponically in perlite at Osnabrück University of Applied Sciences (Osnabrück, Germany). Cultivation took place in a controlled-environment growth chamber maintained at roughly 27 °C and 85% relative humidity, with a 12 h light / 12 h dark photoperiod. Fertilization was provided using Ferty 9 Hydro (Hauert MANNA Düngerwerke GmbH, Nürnberg, Germany) adjusted to an electrical conductivity of 0.8 mS cm^{-1}.

Plant material originated from ca. 30 cm (3-node cuttings) vine cuttings of healthy *V. planifolia* plants aged between 2 and 3 years. Cuttings were pre-cultivated for four months in 80 g perlite substrate (11 cm diameter polyethylene pots) under controlled conditions: 27 ± 0.1 °C, 85 ± 2.9% relative humidity (RH), and a PPFD of 63 µmol m^{-2} s^{-1} (380-750 nm; Valoya LED modules, Finland) with a 12 h photoperiod. Plants received 100 mL tap water weekly without additional fertilisation. The source plants did not visibly differ in vigour after the four-month pre-cultivation, age class was not used as a blocking factor; instead, cuttings were pooled and treated as a single homogeneous source population for the selection process. After pre-cultivation, morphologically uniform and healthy plants were selected for the experiment. Selection criteria were: (i) visibly intact, leaves with no chlorotic, necrotic, or pathogen-related symptoms; (ii) one new shoot developed during pre-cultivation as evidence of active growth; (iii) visually comparable length of the new shoot growth across selected plants. Plants that did not meet all three criteria were excluded.

Experimental design and growth conditions

The experiment followed a completely randomised design with two treatment factors: PPFD (four levels) and NO_3^--N supply (six levels), each replicated with four plants per treatment combination (4 × 6 × 4 = 96 plants). Plants were arranged on a rack (total area 4.1 m^2) divided into four blocks, each equipped with an APOLLO1 TUNEABLE multi-wavelength LED module (FUTURELED, Germany) providing a distinct PPFD treatment: 10, 62, 125 or 208 µmol m^{-2} s^{-1}. The spectral distribution was kept constant across all PPFD levels (Fig. S1). The photoperiod was set to 12/12 h (day/night).

The four PPFD levels were chosen as follows. The lowest level (10 µmol m^{-2} s^{-1}) represents deep shade and reflects the shaded understorey light environment of natural *V. planifolia* habitats [11]. The second level (62 µmol m^{-2} s^{-1}) corresponds to the pre-cultivation irradiance and matches the low-light treatment used for vegetative *Phalaenopsis* [16]. The two highest

levels (125 and 208 µmol m^{-2} s^{-1}) lie well below the irradiance at which photoinhibition has been documented in this species and were chosen to test whether vegetative growth saturates even before reaching the 369-577 µmol m^{-2} s^{-1} range previously reported as optimal under field-relevant midday photosynthetically active radiation (PAR) [13]. Because each PPFD level was supplied by a single dedicated LED module above one shelf, PPFD is confounded with shelf and light source; the four blocks replicate the nitrogen treatments within each PPFD level. The experiment was conducted in a climate-controlled indoor facility, Data loggers in every block showed that the microclimate remained within a 1.2 °C range across PPFD levels. A residual microclimatic contribution to the PPFD confound cannot be ruled out but is acknowledged and addressed in the Discussion.

Within each block, six NO_3^--N supply levels were applied: 6.9, 18.7, 27.5, 37.0, 47.3 and 60.5 mg NO_3^--N L^{-1}, delivered as a hydroponic nutrient solution every 14 days (200 mL per plant). Nitrogen was supplied exclusively as nitrate because ammonium is known to cause rapid pH decline in inert, weakly buffered substrates such as perlite [31]. This choice was made because the optimal substrate pH range reported for *V. planifolia* is 6.0-7.0 [32], and rapid acidification of the perlite root zone driven by NH_4^+ uptake and nitrification would risk pushing the root zone below this optimum within a single application interval [33].

The nutrient solution was formulated to maintain consistent concentrations of all other macro- and micronutrients as far as fertiliser salt stoichiometry permitted; NO_3^--N was the target variable, while SO_4^{2-}-S and Mg co-varied among treatments as a consequence of the fertiliser salt composition. Specifically, SO_4^{2-}-S decreased and Mg increased with NO_3^--N supply (full composition in Fig. S2), so the nitrogen treatment is, strictly speaking, an N-dominated fertilisation gradient rather than a single-variable nitrogen contrast. Because SO_4^{2-}-S and Mg co-varied in opposite directions across the gradient, no single compensating salt could equalise both simultaneously; any corrective addition would have introduced a substitute counter-ion gradient (Cl^-, K^+, or Na^+) and could have also exceeded the EC

range proven compatible with *V. planifolia* in hydroponics [10]. We therefore retained the N-dominated fertilisation gradient framing. Actual NO_3^--N concentrations in prepared solutions were verified by LUFA Nord-West (Oldenburg, Germany; accredited method AA 1/1-522), and remaining element concentrations were confirmed by ICP-OES at Osnabrück University of Applied Sciences [34]. Solution pH was adjusted to 6.68 ± 0.23 before each application using potassium hydroxide. To establish a pre-treatment baseline, all plants received the same nitrogen-free nutrient solution at day 0. Trays were scrubbed in demineralised water two days before each subsequent application of solution.

Four additional pots per block, filled with perlite but containing no plants (dummy pots), received nutrient solutions at the 18.7 and 47.3 mg NO_3^--N L^{-1} levels to distinguish plant-mediated from substrate-mediated effects on leachate parameters. Air temperature was recorded by shielded data loggers placed inside empty pots in each block; an additional logger on top of the substrate captured radiation-induced temperature variation. Mean air temperature across blocks was 26.1 ± 0.5 °C, with Block 4 (208 µmol m^{-2} s^{-1}) recording the highest mean (26.9 °C) and Block 1 (62 µmol m^{-2} s^{-1}) the lowest (25.8 °C, closest to the entrance). Inside the blocks, mean RH was 83.5 ± 1.9% and CO_2 concentration 533 ± 81 ppm. Humidity was supplemented by periodic spraying with demineralised water (pH 6.4 ± 0.3, EC 0.10 ± 0.04 mS cm^{-1}). The experiment lasted 154 days, comprising a 14-day pre-treatment phase (day 0-14) and a 140-day differentiated-PPFD treatment phase (day 14-154). On day 0, all plants received a single nitrogen-free nutrient solution application and remained at PPFD of 62 µmol m^{-2} s^{-1}. From day 14 onward, the four PPFD treatments were imposed and the nutrient solution was applied 10 times at 14-day intervals (days 14, 28, …, 140), with the final 14 days (day 140-154) representing continued growth in the last applied solution before harvest. The spatial arrangement of treatments is shown in Fig. 1.

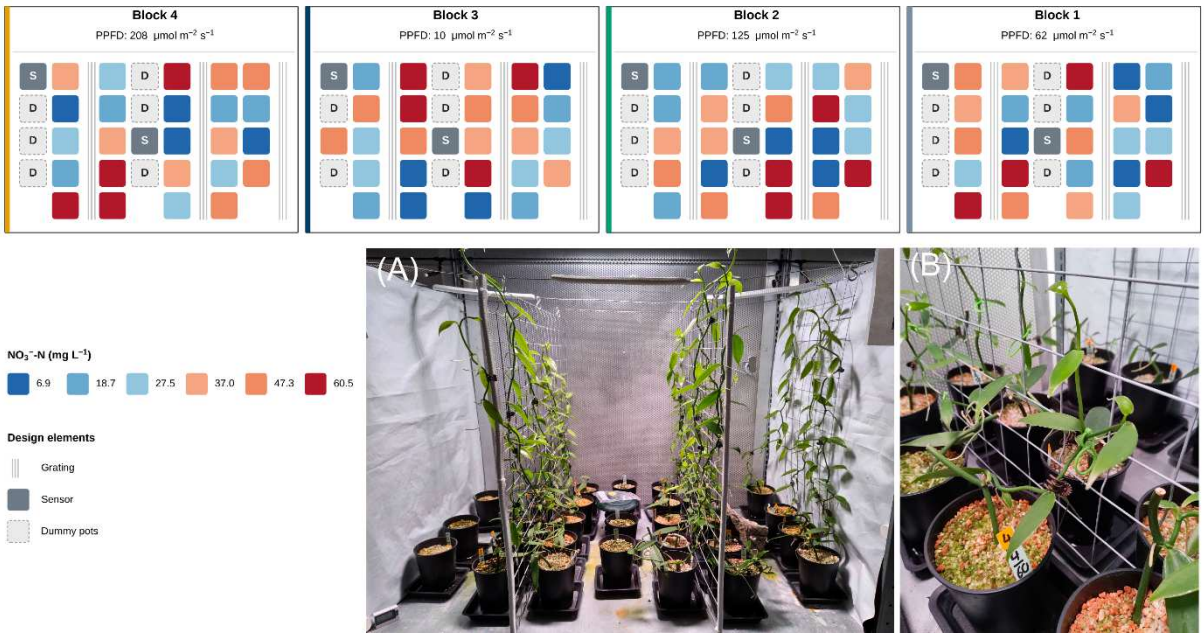

Fig. 1. Randomised design for controlled *Vanilla planifolia* cultivation. Four blocks on separate shelves each received a different PPFD level (10, 62, 125, and 208 µmol m^{-2} s^{-1}). Within each block, six NO_3^--N concentrations (6.9-60.5 mg L^{-1}) were randomly assigned to 24 plants (n = 4), totalling 96 plants. Cell colour indicates NO_3^--N level (blue-to-red scale); grey hatched columns = gratings, dark grey cells = sensors, dashed cells = dummy pots (only substrate). (A) Block 2 at day 120; (B) Closeup of Block 3 at day 60.

Plants were grown throughout pre-cultivation and the experiment in perlite (2-6 mm; pH < 8.5; EC < 100 µS cm^{-1}; nutrient-free; Knauf Performance Materials GmbH, Dortmund, Germany; [35]). Perlite was chosen for its chemically inert nature.

Leachate monitoring

At each nutrient application, leachate was collected in trays below pots as pooled samples per NO_3^--N level within each block. Leachate pH, EC and NO_3^--N concentration (mg L^{-1}) were measured using handheld meters (PH603+K and COND 6+, Eutech Instruments, Singapore) and a Reflectometer RQflex® 20 (Supelco, Germany). Spot checks for NH_4^+-N were performed on selected leachate samples to confirm the absence of ammonium. Inflow nutrient solution was likewise characterised for pH and

EC at every application. All measured nitrate values were converted from NO_3^- to NO_3^--N by dividing by 4.427.

Morphometric and biomass analysis

At 154 days after treatment start (DAT), plants were harvested and separated into leaves, shoots and roots. Morphometric parameters, including shoot length, internode length, leaf area, root length and shoot diameter, were quantified from digital images using ImageJ/Fiji (v1.54p, [36]). At harvest, only newly produced biomass (excluding root biomass) formed during the experimental period was retained for analysis; the initial base material of the cutting/pre-cultivated young plant, marked at the onset of treatment, was identified and excluded prior to weighing. This ensured that biomass and morphometric data reflected growth under the imposed light and nitrogen treatments and were less confounded by tissue produced under the pre-cultivation environment. Derived parameters included specific leaf area (SLA), leaf area ratio (LAR) and root-to-shoot ratio. LAR and root-to-shoot ratio are also computed from de novo biomass only; thus, their absolute values are not directly comparable to those obtained from field-harvested plants, but values support comparisons between treatments. Light use efficiency (LUE) was calculated as total dry mass at harvest divided by the cumulative photon dose received during the 140-day differentiated-PPFD phase (all formulas in Tab. S2). Dry mass was determined after oven-drying at 60 °C to constant mass.

Physiological measurements

Physiological measurements were conducted once, four days before harvest, on standardised leaves of comparable developmental age across all plants. Chlorophyll a fluorescence was measured using a portable pulse-amplitude modulated fluorometer (MINI-PAM II, Heinz Walz GmbH, Effeltrich, Germany). Parameters recorded included maximum quantum yield of photosystem II (PSII; Fv/Fm) after 60 min dark adaptation, effective quantum yield of photosystem II (Y(II)), NPQ and the yield of non-regulated energy dissipation (Y(NO)) under ambient light conditions. Stomatal conductance (g_{sw}; mmol m^{-2} s^{-1}) was measured under both dark-adapted

and light-adapted conditions using a steady-state porometer (SC-1, METER Group, Pullman, WA, USA). Relative chlorophyll content was estimated with a SPAD-502Plus chlorophyll meter (Konica Minolta Inc., Osaka, Japan). All measurements were replicated two to five times per plant depending on data plausibility, and means per plant were used for further analysis, details are provided in Tab. S1.

Elemental analysis

All tissue elemental analyses were performed by SGS Analytics Germany GmbH (Jena, Germany). Dried leaf tissue from the 96 plants was pooled into composite samples because individual plants did not yield sufficient dry mass for reliable elemental determination. At 10 µmol m^{-2} s^{-1} PPFD, the four plants of each NO_3^--N level were combined into a single composite (one sample per N level). At each of the three higher PPFD levels, the four plants per N level were combined in pairs, yielding two composites per N level. Dry matter content was determined according to [37]. Total nitrogen was determined by the Dumas combustion method [38] on all 42 samples. Leaf N is reported as percentage of dry mass. For a subset of 16 samples, macro- and micronutrient concentrations (Ca, Fe, K, Mg, P) were determined by inductively coupled plasma mass spectrometry [39] after HNO_3 pressure digestion [40].

Statistical analysis

For all biomass, morphological, fluorescence, physiological and resource-use parameters normality and homoscedasticity of residuals were assessed via Shapiro-Wilk and Levene's tests. Where violated, data were log- or square-root-transformed; remaining heteroscedastic parameters were analysed with HC3 heteroscedasticity-consistent (estimator type 3) standard errors. Treatment effects were tested by analysis of covariance (ANCOVA; Y ~ Light + poly(N, 2) + Light × poly(N, 2)) with Type II sums of squares and HC3-adjusted *F*-tests. Post-hoc comparisons among PPFD levels used estimated marginal means with Tukey adjustment. Nitrogen dose-response curves within each PPFD level were characterised by second-order polynomial regressions ($Y = \beta_0 + \beta_1 N + \beta_2 N^2$) with HC3

standard errors for four parameters selected from the ANCOVA based on significant nitrogen effects and coverage of distinct physiological dimensions. Nitrogen optima were estimated as $N_{opt} = -\beta_1 / (2\beta_2)$. Tissue nutrient concentrations, which did not meet parametric assumptions, were analysed using Kruskal-Wallis tests with Dunn's post-hoc comparisons and Holm-adjusted *p*-values. All analyses were performed in R v4.5.2 with script development assisted by Claude Opus 4.7 (Anthropic). All output was reviewed and verified by the authors. Statistical workflow, assumption diagnostics, transformation decisions and detailed ANCOVA, regression and Kruskal-Wallis results are provided in Tab. S2. Details on missing values and observations excluded from the analysis are also provided in Tab. S2.

Results

Overview of light intensity and nitrate supply effects

Light intensity was the dominant treatment factor, with significant effects ($p < 0.05$) on 16 of 20 parameters analysed, while NO_3^- supply exerted significant linear effects on 12 (Tab. 1). Significant quadratic responses were limited to root-to-shoot ratio and biomass per N. Light × nitrogen interactions were detected for shoot dry mass, shoot length, root length, and relative chlorophyll content, indicating that the nitrogen dose-response differed among PPFD levels for these parameters. Chlorophyll fluorescence parameters responded exclusively to light, with no significant nitrogen or interaction effects. Effect sizes for all parameters are provided in Tab. S2.

Tab. 1. Effects of photosynthetic photon flux density (PPFD) and NO_3^--N supply on growth, morphology, physiology, and resource use efficiency of *Vanilla planifolia*. Values are means ± SD per PPFD level, pooled across six nitrogen levels (n = 24), except for internode length (n = 22-24), Fv/Fm (n = 22-24), Y(II) (n = 20-24), and NPQ and Y(NO) (n = 18-24). ANCOVA model: Y ~ Light + poly(N, 2) + Light × poly(N, 2) with HC3 robust standard errors. L = PPFD main effect; Nlin = linear nitrogen; Nquad = quadratic nitrogen; L × N = interaction. Different lowercase letters indicate significant differences among PPFD levels (Tukey-adjusted, $p < 0.05$). ns, not significant; *$p < 0.05$; **$p < 0.01$; ***$p < 0.001$. † Transformed prior to analysis; untransformed means displayed.

Parameter	*Light intensity*				*Statistics*			
	10 (µmol m⁻² s⁻¹)	**62** (µmol m⁻² s⁻¹)	**125** (µmol m⁻² s⁻¹)	**208** (µmol m⁻² s⁻¹)	***L***	***N_{lin}***	***N_{quad}***	***L × N***
Total dry mass (g) †	0.311 ± 0.134 a	1.29 ± 0.45 b	1.95 ± 0.65 c	1.97 ± 0.90 c	***	***	ns	ns
Leaf dry mass (g) †	0.088 ± 0.039 a	0.428 ± 0.189 b	0.627 ± 0.237 c	0.614 ± 0.333 bc	***	***	ns	ns
Shoot dry mass (g) †	0.102 ± 0.041 a	0.533 ± 0.192 b	0.713 ± 0.257 b	0.776 ± 0.429 b	***	***	ns	*
Root dry mass (g) †	0.120 ± 0.076 a	0.327 ± 0.119 b	0.614 ± 0.229 c	0.583 ± 0.223 c	***	ns	ns	ns
Root-to-shoot ratio (g g⁻¹) †	0.644 ± 0.420 ab	0.367 ± 0.145 a	0.484 ± 0.158 b	0.526 ± 0.361 b	*	***	*	ns
Shoot length (cm)	27.7 ± 12.8 a	66.5 ± 17.9 b	71.9 ± 19.5 b	71.3 ± 30.9 b	***	***	ns	***
Internode length (cm)	5.10 ± 1.04 a	5.33 ± 0.99 a	5.11 ± 0.66 a	4.91 ± 1.08 a	ns	***	ns	ns
Leaf area (cm²) †	35.7 ± 13.6 a	115.3 ± 40.5 b	149.7 ± 48.7 b	135.8 ± 64.0 b	***	***	ns	ns
SLA (cm² g⁻¹)	439.7 ± 191.9 b	278.4 ± 27.8 b	244.0 ± 19.4 a	230.4 ± 20.6 a	***	***	ns	ns
LAR (cm² g⁻¹)	120.9 ± 31.5 b	89.9 ± 13.6 b	76.8 ± 8.1 a	68.3 ± 10.6 a	***	ns	ns	ns
Root length (cm) †	40.0 ± 19.3 a	122.0 ± 40.6 b	193.5 ± 52.2 c	283.7 ± 114.7 c	***	*	ns	**
Relative chlorophyll content (SPAD)	27.8 ± 4.2 a	23.6 ± 7.3 a	24.9 ± 7.4 a	22.0 ± 8.2 a	***	***	ns	***
Stomatal cond. dark (mmol m⁻² s⁻¹) †	23.3 ± 4.8 a	23.4 ± 10.9 a	21.1 ± 3.9 a	20.4 ± 6.2 a	ns	*	ns	ns
Stomatal cond. light (mmol m⁻² s⁻¹) †	23.4 ± 6.4 a	23.0 ± 3.9 a	21.6 ± 5.9 a	22.0 ± 4.4 a	ns	ns	ns	ns
F_v/F_m (dark)	0.759 ± 0.037 b	0.733 ± 0.038 a	0.716 ± 0.044 ab	0.686 ± 0.085 a	***	ns	ns	ns
Y(II)	0.772 ± 0.026 c	0.708 ± 0.073 b	0.637 ± 0.101 b	0.540 ± 0.113 a	***	ns	ns	ns
NPQ	0.077 ± 0.091 a	0.530 ± 0.594 abc	0.785 ± 0.631 b	1.54 ± 1.20 c	***	ns	ns	ns
Y(NO)	0.213 ± 0.029 a	0.204 ± 0.043 a	0.216 ± 0.052 a	0.208 ± 0.078 a	ns	ns	ns	ns
LUE (g (mol m⁻²)⁻¹) †	0.0051 ± 0.0022 d	0.0034 ± 0.0012 c	0.0026 ± 0.0009 b	0.0016 ± 0.0007 a	***	ns	ns	ns

Parameter	*Light intensity*				*Statistics*			
	10 (µmol m^{-2} s^{-1})	**62** (µmol m^{-2} s^{-1})	**125** (µmol m^{-2} s^{-1})	**208** (µmol m^{-2} s^{-1})	***L***	***N_{lin}***	***N_{quad}***	***L × N***
Biomass per N (g (mg L^{-1})$^{-1}$) †	0.016 ± 0.018 a	0.057 ± 0.046 b	0.080 ± 0.048 c	0.077 ± 0.047 c	***	***	***	ns

393

394 *Biomass accumulation and allocation*

395 Total dry mass differed among PPFD levels, increasing more than sixfold
396 from 0.31 ± 0.13 g at 10 to 1.95 ± 0.65 g at 125 µmol m^{-2} s^{-1} ($p < 0.001$,
397 $\eta^2 p = 0.79$), while 125 and 208 µmol m^{-2} s^{-1} did not differ statistically (Tab.
398 1). Nitrogen had a positive linear effect ($p < 0.001$) but no quadratic
399 component was detected. The biomass fractions diverged in their
400 responses: root dry mass increased with PPFD ($p < 0.001$) but showed no
401 statistically supported nitrogen response ($p = 0.08$), while shoot dry mass
402 responded to both factors, with a light × nitrogen interaction ($p = 0.048$)
403 indicating that the nitrogen response of shoot growth depended on PPFD
404 level. The root-to-shoot ratio was lowest at 62 µmol m^{-2} s^{-1}, higher at 125
405 and 208, and intermediate at 10 µmol m^{-2} s^{-1} (group ab; Tab. 1); it showed
406 both linear ($p < 0.001$) and quadratic ($p = 0.03$) nitrogen effects, suggesting
407 a non-linear shift in allocation with increasing nitrogen supply. LUE declined
408 monotonically across the PPFD gradient (Tab. 1; $p < 0.001$), with all four
409 light levels statistically separated.

410

411 ***Morphometric responses***

412 Shoot length increased 2.4-fold from 10 to 62 µmol m^{-2} s^{-1} but did not differ
413 statistically among the three higher PPFD levels ($p < 0.001$ for light; light ×
414 nitrogen interaction $p < 0.001$). In contrast, internode length was unaffected
415 by PPFD but responded linearly to nitrogen ($p < 0.001$), indicating that the
416 additional shoot length at higher PPFD arose from more internodes rather
417 than longer ones. Leaf area was 3.7-fold greater at the three higher PPFD
418 levels than at 10 µmol m^{-2} s^{-1} ($p < 0.001$), with no statistical differences
419 among 62, 125, and 208. SLA and LAR both declined with increasing PPFD
420 and shared the same two-group pattern: values at 10 and 62 were
421 numerically different but not statistically distinguishable, while both were
422 higher than at 125 and 208 µmol m^{-2} s^{-1} (Tab. 1). Root length increased

stepwise from 10 through 62 to 125 µmol m^{-2} s^{-1} (40 to 122 to 194 cm; $p < 0.001$). At 208 µmol m^{-2} s^{-1}, root length increased by nearly half again (284 ± 115 cm), but this 47% increase over the 125 level was not statistically supported ($p = 0.059$), likely because the high variability at the highest PPFD reduced statistical power for this comparison. Notably, the overall light effect on root length was large ($\eta^2p = 0.77$; Tab. S2). A light × nitrogen interaction was also present ($p = 0.004$).

Leaf physiology and chlorophyll fluorescence

Maximum quantum yield of photosystem II (PSII) (Fv/Fm) declined from 0.759 ± 0.037 at 10 to 0.686 ± 0.085 at 208 µmol m^{-2} s^{-1} ($p < 0.001$); post-hoc separation placed the 10 µmol m^{-2} s^{-1} level above 62 and 208, while 125 was intermediate (Tab. 1). Effective quantum yield Y(II) decreased from 0.772 ± 0.026 to 0.540 ± 0.113 across the same gradient ($p < 0.001$), with all four light levels separated except 62 and 125, which did not differ. NPQ rose from 0.077 ± 0.091 at 10 to 1.54 ± 1.20 at 208 µmol m^{-2} s^{-1} ($p < 0.001$). None of the fluorescence parameters showed a statistically supported nitrogen or interaction effect.

Relative chlorophyll content (SPAD) of young leaves showed a strong linear nitrogen effect ($p < 0.001$) and a significant light × nitrogen interaction ($p < 0.001$). The pooled light means did not differ in post-hoc comparisons (Tab. 1), indicating that the light effect on SPAD depended on nitrogen supply. Dark-adapted stomatal conductance (g_{sw}) showed a weak negative linear nitrogen effect ($p = 0.036$) but did not differ significantly among PPFD levels. Light-adapted g_{sw} was not significantly affected by either treatment.

Nitrogen dose-response relationships

Biomass per N showed the most consistent dose-response across all PPFD levels (R^2adj = 0.52-0.81; Fig. 2, panel B). The estimated nitrogen optima for biomass per N fell within a narrow range of 50-56 mg NO_3^--N L^{-1}; the quadratic coefficient was significant at 10, 62, and 125 µmol m^{-2} s^{-1} ($p < 0.05$) and marginally non-significant at 208 µmol m^{-2} s^{-1} ($p = 0.07$).

No significant light × nitrogen interaction was detected for this parameter in the ANCOVA.

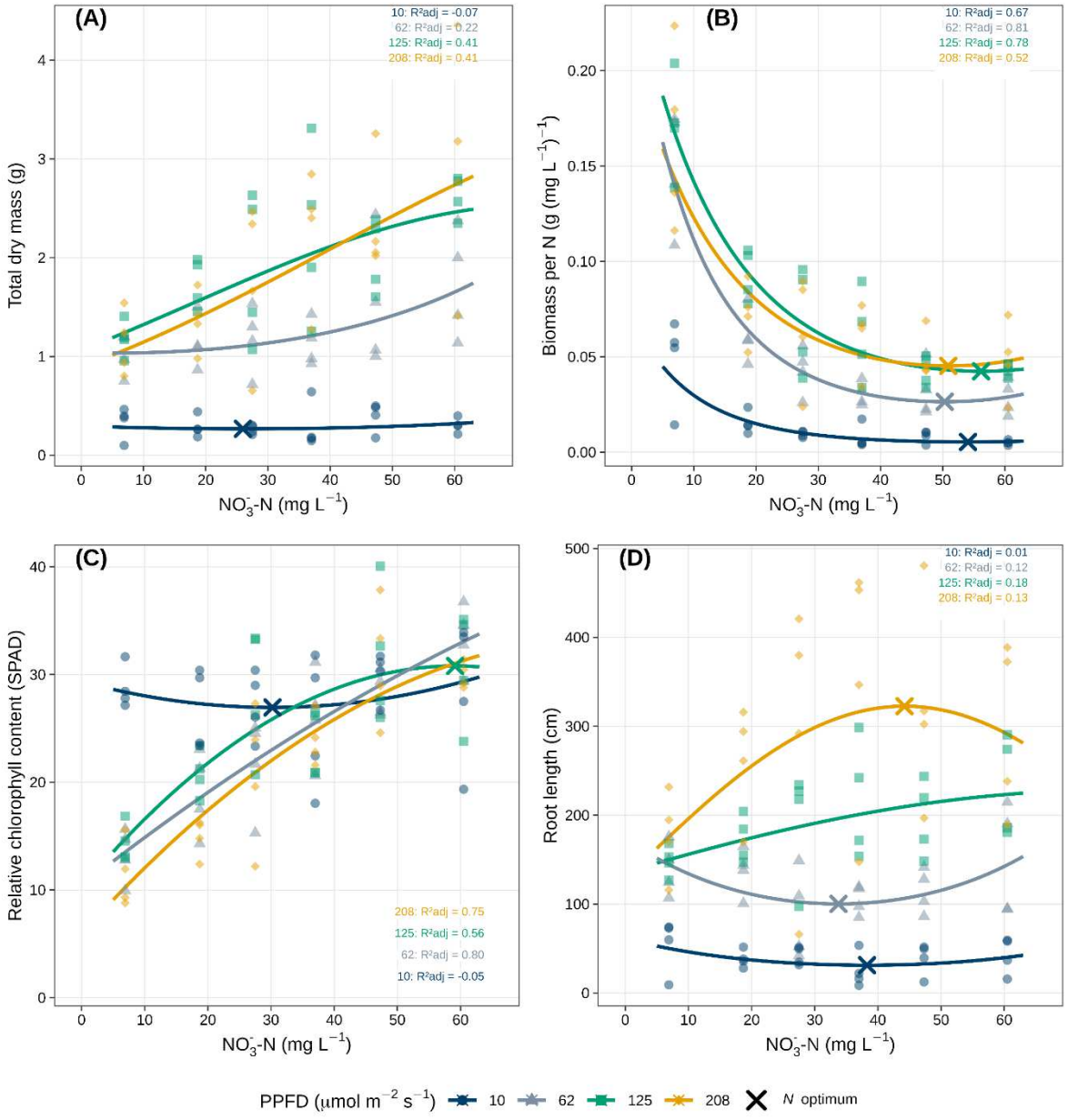

Fig. 2. Nitrogen dose-response curves for (A) total dry mass, (B) biomass per N, (C) relative chlorophyll content (SPAD), and (D) root length of *V. planifolia* grown at four PPFD levels (n = 24 per PPFD level; n = 96 total). Lines represent second-order polynomial regressions fitted within each PPFD level with HC3 standard errors. × symbols indicate estimated nitrogen optima ($N_{opt} = -\beta_1/2\beta_2$) where the quadratic coefficient was significant. R^2_{adj} values are shown per PPFD level.

For total dry mass, the polynomial fit improved with increasing PPFD (R^2_{adj} = −0.07 at 10 vs. 0.41 at both 125 and 208 µmol m^{-2} s^{-1}; individual regression coefficients were not significant at 10). SPAD was well predicted by nitrogen at 62, 125, and 208 µmol m^{-2} s^{-1} (R^2_{adj} = 0.56-0.80; β_1 significant at $p < 0.01$) but not at 10 µmol m^{-2} s^{-1} (R^2_{adj} = −0.05). Root length was weakly predicted by nitrogen across all PPFD levels ($R^2_{adj} \leq$ 0.18).

Leaf nitrogen content

Leaf nitrogen ranged from 1.0 to 2.4% dry mass across all treatment combinations (Fig. 3). Leaf N concentration differed significantly among nitrogen supply levels, increasing from 1.28 ± 0.33% dry mass at 6.9 mg NO_3^--N L^{-1} to 2.18 ± 0.08% dry mass at 47.3 mg NO_3^--N L^{-1}, with no further increase at 60.5 mg NO_3^--N L^{-1}. Dunn's post-hoc test (Holm-corrected) confirmed that the two highest supply levels (47.3 and 60.5 mg NO_3^--N L^{-1}) differed significantly from the three lowest levels (6.9, 18.7 and 27.5 mg NO_3^--N L^{-1}); the lowest supply level (6.9 mg NO_3^--N L^{-1}) additionally differed from 37 mg NO_3^--N L^{-1}. The plateau at 2.1-2.2% dry mass at 47-60 mg NO_3^--N L^{-1} is consistent with the N-use-efficiency optimum identified for biomass per N in the ANCOVA (Tab. 1) and suggests saturation of nitrogen accumulation capacity at higher supply rates. Values from all four PPFD levels overlapped closely at most nitrogen levels, and light intensity had no significant effect on leaf N concentration. However, given the limited sample sizes across PPFD levels, this observation should be interpreted with caution. Detailed statistical results, including post-hoc comparisons and effect sizes, are provided in Tab. S2. Leaf tissue concentrations of Ca, Fe, K, Mg, and P are provided in Fig. S3.

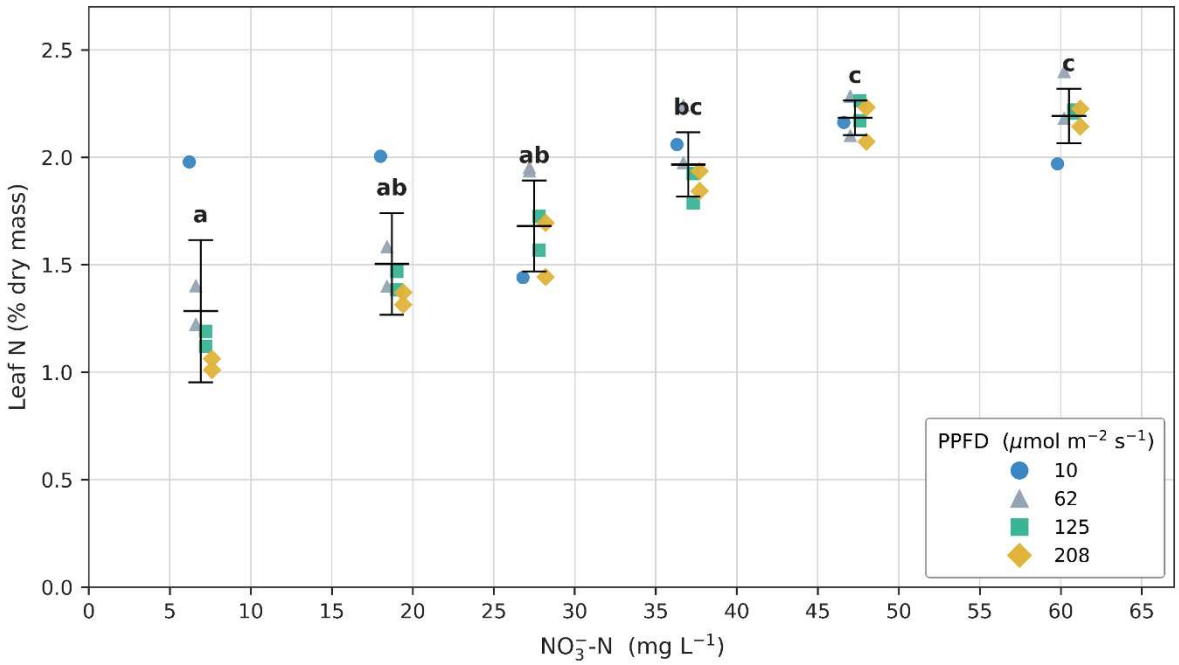

Fig. 3. Leaf nitrogen concentration (% dry mass) of *Vanilla planifolia* after 154 days of treatment as a function of NO_3^--N supply (mg L^{-1}). Each point represents one composite leaf sample pooled from 4 plants at 10 µmol m^{-2} s^{-1} or 2 plants at the higher PPFD levels, coloured by photosynthetic photon flux density (PPFD; µmol m^{-2} s^{-1}): 10 (circle), 62 (triangle), 125 (square), and 208 (diamond). Horizontal bars indicate the mean across all PPFD levels at each N dose; whiskers show ± SD (n = 7 composite samples per N level). Lowercase letters denote significant differences among N levels (Kruskal–Wallis $H(5) = 30.6$, $p < 0.001$; Dunn's post-hoc test, Holm-corrected, $\alpha = 0.05$); NO_3^--N supply levels sharing a letter do not differ significantly.

Leachate dynamics

Leachate NO_3^--N concentration generally tracked the applied nutrient solution levels throughout the 140-day monitoring period (Fig. 4, panel A). At the highest supply level (60.5 mg NO_3^--N L^{-1}), leachate NO_3^--N reached around 60-80 mg L^{-1} during mid-experiment. At intermediate supply levels, leachate nitrogen values stabilised or showed a declining trend over time. At the two lowest supply levels, leachate NO_3^--N remained below 25 mg L^{-1} throughout.

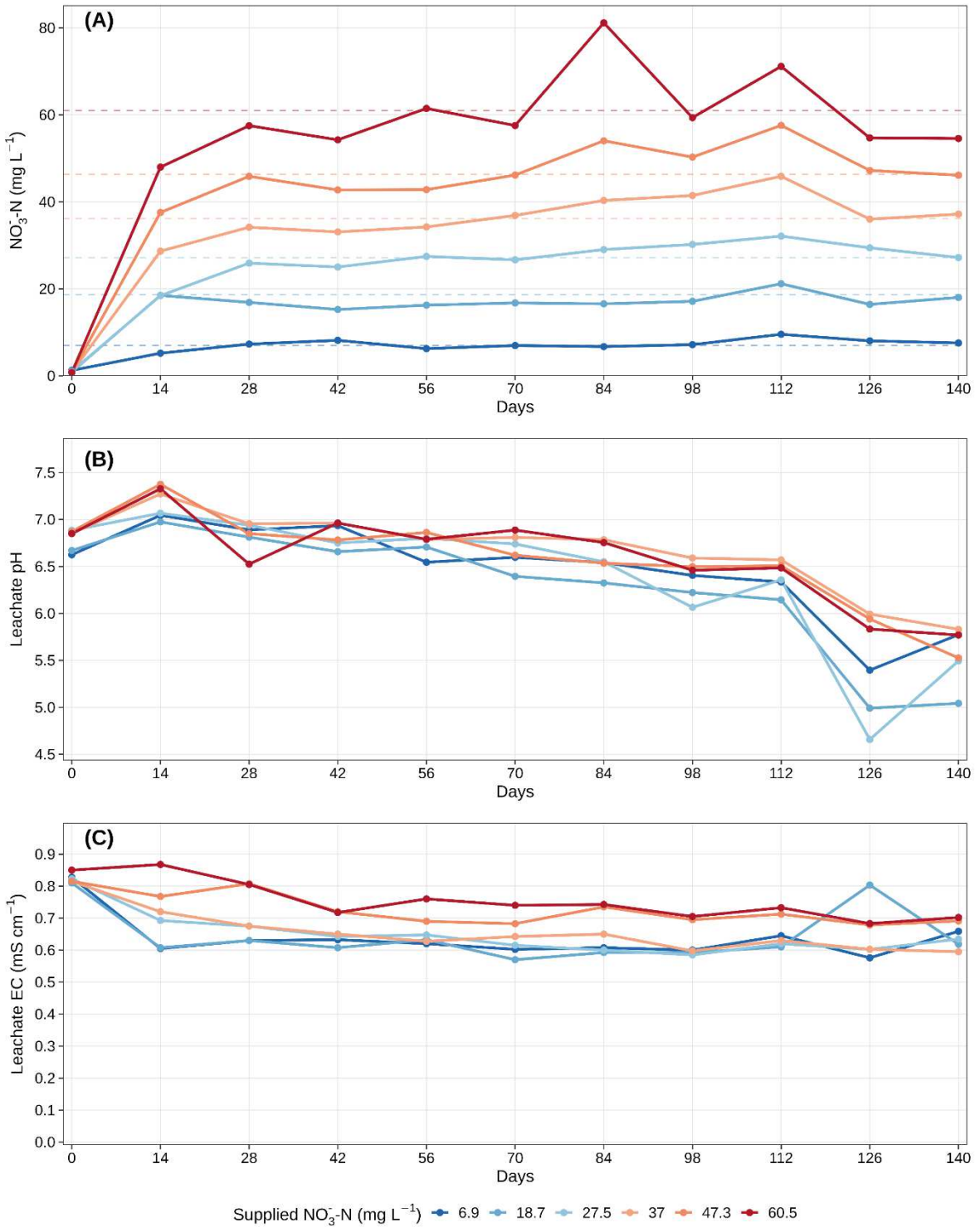

516

517 **Fig. 4.** Temporal dynamics of leachate (A) NO_3^--N concentration, (B) pH,
518 and (C) electrical conductivity (EC) over 140 days of *Vanilla planifolia*
519 cultivation in perlite substrate under six NO_3^--N supply levels. At day 0, all
520 treatments received a nitrogen-free nutrient solution containing all other
521 essential nutrients as a pre-treatment. Data points represent means across
522 four PPFD levels; leachate within each PPFD level was pooled across four

replicate plants per nitrogen level. Nutrient solutions were applied every 14 days.

Leachate pH declined from initial values near 6.8-7.0 to around 5.0-5.5 by 140 DAT across most treatments (Fig. 4, panel B), despite the inflow solution being adjusted to around pH 7.0 before each application. The pH decline was broadly uniform across nitrogen levels. Leachate EC fluctuated between 0.6 and 0.9 mS cm^{-1} over the course of the experiment, with moderate temporal peaks (Fig. 4, panel C). Comparison between dummy and plant pots for leachate (pH and NO_3-N) is shown in Fig. S4.

Discussion

The saturation of dry mass gain at 125 µmol m^{-2} s^{-1} is consistent with the understorey ecology of *V. planifolia*, which naturally grows beneath the forest canopy under moderate shade conditions [11]. A comparable optimum has been reported for *V. planifolia* at intermediate relative illumination around 8.6-12.8 mol m^{-2} d^{-1} PAR [13]. Together, these findings suggest a practical PPFD threshold near 125 µmol m^{-2} s^{-1} (DLI ≈ 5.4 mol m^{-2} d^{-1}) for vegetative biomass accumulation under a 12 h photoperiod, while optimal growth under field conditions with natural spectral composition may require somewhat higher DLIs (8.6-12.8 mol m^{-2} d^{-1}; [13]). By comparison, *Phalaenopsis* showed only 21 to 30% total dry mass and 41 to 55% root dry mass gains across a similar PPFD range of 60 to 140 µmol m^{-2} s^{-1} [16], whereas *V. planifolia* gained 51% and 88% respectively between 62 and 125 µmol m^{-2} s^{-1}. Within the specific experimental setup tested here, *V. planifolia* therefore appears more responsive to additional light than its closest studied CAM orchid comparator. Each PPFD level was supplied by one LED module above one shelf, so shelf position, microclimate (up to 1.2 °C between blocks) and LED unit are confounded with PPFD; block-level replication remains valid for the nitrogen treatments and the nitrogen × PPFD interactions. The large light effect sizes (η^2p up to 0.79; Tab. S2), agreement with previous studies [13] and the plausibility of the fluorescence trends support the qualitative direction of the light findings, but the absolute saturation PPFD is best

treated as preliminary until reproduced in an independently replicated light design.

The near-halving of SLA across the PPFD gradient indicates a pronounced shift towards structurally reinforced, thicker leaves at higher light intensity, a classic sun-shade acclimation response [20]. Shoot length increased significantly with PPFD while internode length remained unaffected, implying that additional shoot extension resulted from the production of more phytomers rather than from internodal elongation. This contrasts with the shade-avoidance syndrome of heliophilic species, in which reduced light triggers pronounced internode elongation at the expense of leaf development [41,42].

While Internode length was unaffected by PPFD, it responded linearly to nitrogen supply (Tab. 1). A plausible interpretation is that internode elongation in this shade-tolerant hemiepiphyte is not driven by light intensity within the range tested here, consistent with the suppressed shade-avoidance response in shoot extension reported above; instead, it appears to be limited by nitrogen availability. Nitrogen-driven stem elongation linked to upregulation of cell-wall-formation pathways has been demonstrated in other species [43]. Within a substrate-limited regime, an approximately linear response across a moderate concentration range is expected, and the absence of a quadratic term suggests that the upper plateau lies beyond the highest level tested.

Chlorophyll fluorescence data are consistent with *V. planifolia* acclimated to increasing light intensity, with photoprotective downregulation at the highest PPFD. Healthy autotrophic plants typically show dark-adapted Fv/Fm around 0.79-0.83 [44], with values down to ~0.70 still reported under non-pathological stress [45]. The 0.69 observed at the highest PPFD is below this optimal range but consistent with the status of *V. planifolia* as an obligate shade plant [13]. Since 208 µmol m^{-2} s^{-1} remains far below the irradiance at which chronic photoinhibition has been documented in this species (1285 µmol m^{-2} s^{-1}; [13]), the modest decline from 0.76 at the

lowest PPFD to 0.69 at the highest is best interpreted as acclimative photoprotective downregulation rather than chronic damage. More strikingly, NPQ increased approximately 20-fold across the PPFD gradient, while the quantum yield of non-regulated energy dissipation, Y(NO), remained constant at around 0.21 and showed no significant response to any treatment factor. This pattern is consistent with regulated photoprotective processes (such as the xanthophyll cycle) handling the additional excitation energy without a measurable rise in non-regulated dissipation, although a single-timepoint measurement cannot directly attribute it to a specific mechanism [46].

Thermal energy dissipation via NPQ is not the only photoprotective mechanism available to this species; *V. planifolia* also repositions its chloroplasts away from high-intensity light through a blue-light-mediated avoidance response, as demonstrated by [47]. Notably, none of the fluorescence parameters responded to nitrogen supply or to the light × nitrogen interaction, indicating that PSII acclimation in *V. planifolia* appears to be driven predominantly by irradiance rather than by nitrogen status under these conditions.

Nitrogen supply had significant linear effects on dry mass accumulation and several morphological parameters, yet the nitrogen dose-response was quantitatively secondary to light. Before interpreting the nitrogen response in greater depth, it must be acknowledged that Mg and SO_4^{2-}-S co-varied with NO_3^--N due to fertiliser salt stoichiometry, and the observed responses cannot be unambiguously attributed to nitrogen alone. However, both ions remained within ranges considered sufficient for plant growth [48,49] and below concentrations reported to inhibit growth in hydroponic systems [50,51], making a major confounding effect unlikely. Within-PPFD polynomial regressions identified a narrow optimum of 50-56 mg NO_3^--N L^{-1} for dry mass production efficiency (biomass per N), and this optimum was remarkably stable across PPFD levels. It should be emphasised that the 50-56 mg L^{-1} value reflects peak N-use efficiency, not peak absolute biomass; the linear ANCOVA response of total dry mass to N implies further biomass gains are possible at higher supply, at lower efficiency. Leaf

nitrogen reached approximately 2.1-2.2% dry mass at the highest supply levels, though this estimate is based on a limited number of composite samples and should be interpreted with caution. These values fall within the range of leaf N concentrations reported for *V. planifolia* grown in organic substrates (1.9-2.5% dry mass; [24]) but appear to be lower than the optimal foliar N concentration of 2.3-2.8% dry mass reported for *Phalaenopsis* [27]. This comparatively low saturation point may reflect the hemiepiphytic adaptation of *V. planifolia* to nutrient-poor substrates in tropical forests, where nitrogen availability is typically limiting and plants are adapted to conservative nutrient cycling [52].

The convergence of the nitrogen optimum at 50-56 mg L^{-1} across nearly the entire PPFD range is a notable finding, as it implies that a single fertigation target can serve across the broad range of light environments tested here. This is practically advantageous because it simplifies fertilisation management, although, the target should ideally be validated in larger production systems before being treated as a definitive recommendation. The failure of the polynomial model at 10 µmol m^{-2} s^{-1} ($R^2_{adj} \approx 0$ for total dry mass and SPAD) confirms that light, not nitrogen, was the primary growth-limiting factor at this irradiance: additional nitrogen could not be utilised productively when carbon fixation was constrained by extreme light limitation.

The scarcity of significant light × nitrogen interactions within the tested PPFD and nitrogen ranges suggests a weak coupling between the two factors in *V. planifolia*. In C_3 crops, such interactions are typically more pervasive because higher irradiance increases the demand for nitrogen through greater photosynthetic carbon fixation and chlorophyll turnover [19,53]. In *V. planifolia*, however, intrinsic constraints of CAM biochemistry may decouple nitrogen demand from the light gradient within the PPFD range tested. These constraints plausibly include the limitation of daytime carbon gain by the nocturnal malate pool [12], as well as the low photosynthetic capacity characteristic of the shade-obligate niche. This weak coupling between light and nitrogen has not been reported for *V.*

planifolia before, but it aligns with the general expectation for shade-adapted CAM species [54].

Leaf nitrogen content showed no significant response to PPFD, though this result should be interpreted cautiously given the limited number of composite samples analysed. In contrast, SPAD values exhibited a pronounced light × nitrogen interaction. At 10 µmol m^{-2} s^{-1}, SPAD remained near 28 across all nitrogen levels, whereas at the three higher PPFD levels values ranged from 10-15 at the lowest nitrogen supply to 30-35 at the highest. Because SPAD primarily reflects leaf chlorophyll concentration rather than total nitrogen content [55] these patterns suggest that chlorophyll allocation, rather than overall nitrogen status, was most sensitive to the interaction between light and nitrogen supply. Moreover, the substantially higher SLA at 10 µmol m^{-2} s^{-1} implies thinner leaves, which can reduce SPAD sensitivity independently of actual chlorophyll or nitrogen content [56]. The within-PPFD regressions yielded high predictive power for SPAD at 62 (R^2_{adj} = 0.80) and 208 µmol m^{-2} s^{-1} (R^2_{adj} = 0.75), suggesting that SPAD readings can serve as a practical, non-destructive N-status monitoring tool for growers, provided that light intensity is adequate.

In conclusion, this study strongly indicates that light intensity is the dominant treatment factor for vegetative growth in *V. planifolia*, with dry mass gain saturating near 125 µmol m^{-2} s^{-1} PPFD (DLI ≈ 5.4 mol m^{-2} d^{-1}), while nitrogen supply optimises dry mass production efficiency at 50-56 mg NO_3^--N L^{-1}. The scarcity of significant light × nitrogen interactions suggest that a single fertilisation target may apply across the PPFD range tested in this experiment. These findings were obtained on young, vegetatively growing plants in a controlled hydroponic perlite-based system over 154 days of cultivation; validation across older plants and the reproductive phase is needed before full production protocols can be derived. Nonetheless, the threshold and quantitative dose-response relationships established here provide an evidence-based foundation for optimising *V.*

planifolia cultivation across both traditional and more controlled cultivation systems.

Declarations

Acknowledgement

We would like to thank Justus Wiese and Samuel Eggers, for their excellent technical assistance.

We thank Symrise, project partner in SustainVanil, part of the Innovationsraum NewFoodSystems, for their contributions to our study, including the sourcing of vanilla plant material in compliance with the Nagoya Protocol. In particular, we thank Esther-Corinna Schwarze and Jakob P. Ley for their expertise and support.

The authors used Claude Opus 4.7 (Anthropic, 2026) to assist with R script development for statistical analysis and data visualisation, and for AI-assisted copy editing (grammar, spelling, and stylistic refinement). All output was reviewed and verified by the authors, who retain full responsibility for the manuscript.

Supplementary data

Fig. S1: Light environment
Fig. S2: Nutrient solutions
Fig. S3: Elemental concentrations
Fig. S4: Dummy vs. plant pot comparison
Tab. S1: Measurement details
Tab. S2: Statistical workflow, details, formula and effect size

Author contribution statement

M. V.: Conceptualization, Methodology, Investigation, Formal Analysis, Data Curation, Visualization, Writing - Original Draft and Writing - Review & Editing.

J. v. S.: Conceptualization, Methodology & Writing - Review & Editing.
A. J.: Methodology & Writing - Review & Editing.
F. P.: Conceptualization, Methodology & Writing - Review & Editing.
A. U.: Supervision, Writing - Review & Editing, Project Administration and Funding acquisition.

Corresponding author
Correspondence to Marvin Vahl (m.vahl@hs-osnabrueck.de)

Competing interests
The authors declare that they have no known competing financial interests or personal relationships that could have appeared to influence the work reported in this paper.

Ethics approval
All procedures complied with the regulations of the German government for the collection of biological material for scientific purposes. Experimental research on cultivated plants, including the collection of plant material, was carried out in accordance with all applicable institutional, national, and international guidelines and legislation throughout the course of this study.

This article does not contain any studies with human participants or animals performed by any of the authors.

Funding
This work was supported by the German Federal Ministry of Research, Technology and Space (BMFTR) [grant numbers 031B1238A] under the funding measure Innovation Spaces Bioeconomy (Innovation Space NewFoodSystems) as part of the National Research Strategy BioEconomy 2030.

Data availability

The datasets generated during the current study are available from the corresponding author on reasonable request.

References

1. Havkin-Frenkel D, Belanger FC, editors. Handbook of vanilla science and technology. Second edition. Hoboken, NJ, USA: Wiley; 2018.

2. FAO. FAOSTAT [Internet]. Crops and livestock products. 2026. https://www.fao.org/faostat/en/#data/QCL. Accessed 5 Mar 2026.

3. Khan K, Su C-W, Khurshid A, Umar M. Are there bubbles in the vanilla price? Agric Econ. 2022;10(1):6. https://doi.org/10.1186/s40100-022-00213-y

4. Hänke H. 2024 Living Income Reference Price Update for vanilla sourced from Madagascar [Internet]. Bonn, Germany: Fairtrade International; 2024 pp. 1–49. https://www.fairtrade.net/content/dam/fairtrade/fairtrade-international/library/2024/living-income-reference-prices-for-vanilla-from-uganda-and-madagascar/Fairtrade-Vanilla-Living-Income-Ref-Price-Madagascar-report-2024.pdf Accessed 23 Mar 2026.

5. Koyyappurath S, Atuahiva T, Le Guen R, Batina H, Le Squin S, Gautheron N, et al. Fusarium oxysporum f. sp. radicis-vanillae is the causal agent of root and stem rot of vanilla. Plant Pathology. 2016;65(4):612–25. https://doi.org/https://doi.org/10.1111/ppa.12445

6. Xiong W, Zhao Q, Xue C, Xun W, Zhao J, Wu H, et al. Comparison of Fungal Community in Black Pepper-Vanilla and Vanilla Monoculture Systems Associated with Vanilla Fusarium Wilt Disease. Front Microbiol. 2016;7:117. https://doi.org/10.3389/fmicb.2016.00117

7. Watteyn C, Fremout T, Karremans AP, Huarcaya RP, Azofeifa Bolaños JB, Reubens B, et al. Vanilla distribution modeling for conservation and sustainable cultivation in a joint land sparing/sharing concept. Ecosphere. 2020;11(3):e03056. https://doi.org/10.1002/ecs2.3056

8. Barragán-Ocaña A, Silva-Borjas P, Cecilio-Ayala E. Vanilla production in the world and Mexico: Market value and technology. Social Sciences & Humanities Open. 2024;10:101076. https://doi.org/10.1016/j.ssaho.2024.101076

9. Rahman KU, Thaleth MKB, Kutty GM, Subramanian R. Pilot scale cultivation and production of Vanilla *planifolia* in the United Arab Emirates. Bulgarian Journal of Agricultural Science. 2019;25(6):1143–50.

10. Vahl M, Soukup ST, Beer F, Weinert CH, Petersen F, Kulling SE, et al. Influence of hydroponic cultivation subsystems on vegetative growth, vigour, and metabolite profiles in vanilla. The Journal of Horticultural Science and Biotechnology. 2025;1–17.

11. Fouché JG, Jouve L. Vanilla *planifolia*: history, botany and culture in Reunion island. Agronomie. 1999;19(8):689–703. https://doi.org/10.1051/agro:19990804

12. Lüttge U. Ecophysiology of Crassulacean Acid Metabolism (CAM). Ann Bot. 2004;93(6):629–52. https://doi.org/10.1093/aob/mch087

13. Díez MC, Moreno F, Gantiva E. Effects of light intensity on the morphology and CAM photosynthesis of Vanilla *planifolia* Andrews. Rev Fac Nac Agron. 2017;70(1):8023–33. https://doi.org/10.15446/rfna.v70n1.61736

14. Sanchez F, Bassil E, Crane JH, Shahid MA, Vincent CI, Schaffer B. Spectral light distribution affects photosynthesis, leaf reflective indices, antioxidant activity and growth of Vanilla *planifolia*. Plant Physiology and Biochemistry. 2022;182:145–53. https://doi.org/10.1016/j.plaphy.2022.04.020

15. Wang H, Wang X-Q, Zeng Z-L, Yu H, Huang W. Photosynthesis under fluctuating light in the CAM plant Vanilla *planifolia*. Plant Science. 2022;317:111207. https://doi.org/10.1016/j.plantsci.2022.111207

16. van Tongerlo E, van Ieperen W, Dieleman JA, Marcelis LFM. Vegetative traits can predict flowering quality in Phalaenopsis orchids despite large genotypic variation in response to light and temperature. PLoS ONE. 2021;16(5):e0251405. https://doi.org/10.1371/journal.pone.0251405

17. Hogewoning SW, van den Boogaart SAJ, van Tongerlo E, Trouwborst G. CAM-physiology and carbon gain of the orchid Phalaenopsis in response to light intensity, light integral and CO2. Plant, Cell & Environment. 2021;44(3):762–74. https://doi.org/10.1111/pce.13960

18. Kim JY, Im NH, Shim SY, Lee HB. Photosynthetic acclimation of crassulacean acid metabolism orchid Phalaenopsis in response to light level. Sci Rep. 2025;15(1):13016. https://doi.org/10.1038/s41598-025-96167-4

19. Evans JR. Photosynthesis and nitrogen relationships in leaves of C3 plants. Oecologia. 1989;78(1):9–19. https://doi.org/10.1007/BF00377192

20. Poorter H, Niinemets Ü, Ntagkas N, Siebenkäs A, Mäenpää M, Matsubara S, et al. A meta-analysis of plant responses to light intensity for 70 traits ranging from molecules to whole plant performance. New Phytologist. 2019;223(3):1073–105. https://doi.org/10.1111/nph.15754

21. Petrolli R, Selosse M-A, Bonillo C, Griveau C, Lalanne-Tisné G, Comes B, et al. Mycorrhizal communities of Vanilla *planifolia* in an introduction area (La Réunion) under varying cultivation practices. PLANTS, PEOPLE, PLANET. 2024;6(3):683–96. https://doi.org/10.1002/ppp3.10476

22. Sujatha S, Bhat R. Response of vanilla (*Vanilla planifolia* A.) intercropped in arecanut to irrigation and nutrition in humid tropics of India. Agricultural Water Management. 2010;97(7):988–94. https://doi.org/10.1016/j.agwat.2010.01.031

23. Osorio AI, Osorio NW, Diez MC, Moreno FH. Effects of Organic Substrate Composition, Fertilizer Dose, and Microbial Inoculation on Vanilla Plant Nutrient Uptake and Growth. Acta Hortic. 2012;(964):135–42. https://doi.org/10.17660/ActaHortic.2012.964.17

24. Osorio AI, Vega NWO, Diez MC, Moreno FH. Nutrient status and vegetative growth of Vanilla *planifolia* Jacks plants as affected by fertilization and organic substrate composition. Acta Agronómica. 2014;63(4):326–34.

841 25. Diez MC, Osorio NW, Moreno F. Effect of dose and type of fertilizer on
842 flowering and fruiting of vanilla plants. Journal of Plant Nutrition.
843 2016;39(9):1297–310. https://doi.org/10.1080/01904167.2015.1098673

844 26. Bichsel RG, Starman TW, Wang Y-T. Nitrogen, Phosphorus, and Potassium
845 Requirements for Optimizing Growth and Flowering of the Nobile Dendrobium as
846 a Potted Orchid. HortScience. 2008;43(2):328–32.
847 https://doi.org/10.21273/HORTSCI.43.2.328

848 27. Mantovani C, Prado R de M, Pivetta KFL. Foliar diagnosis in Phalaenopsis
849 orchid plants subjected to application of nitrogen. AJAR. 2015;10(53):4906–12.
850 https://doi.org/10.5897/AJAR2015.9921

851 28. Wang Y-T, Chang Y-CA. Effects of Nitrogen and the Various Forms of Nitrogen
852 on Phalaenopsis Orchid—A Review. HortTechnology. 2017;27(2):144–9.
853 https://doi.org/10.21273/HORTTECH03204-16

854 29. Veresoglou SD, Barto EK, Menexes G, Rillig MC. Fertilization affects severity of
855 disease caused by fungal plant pathogens. Plant Pathology. 2013;62(5):961–9.
856 https://doi.org/10.1111/ppa.12014

857 30. Kwon MJ, Hwang Y, Lee J, Ham B, Rahman A, Azam H, et al. Waste nutrient
858 solutions from full-scale open hydroponic cultivation: Dynamics of effluent quality
859 and removal of nitrogen and phosphorus using a pilot-scale sequencing batch
860 reactor. J Environ Manage. 2021;281:111893.
861 https://doi.org/10.1016/j.jenvman.2020.111893

862 31. Cytryn E, Levkovitch I, Negreanu Y, Dowd S, Frenk S, Silber A. Impact of short-
863 term acidification on nitrification and nitrifying bacterial community dynamics in
864 soilless cultivation media. Appl Environ Microbiol. 2012;78(18):6576–82.
865 https://doi.org/10.1128/AEM.01545-12

866 32. Mayorga Pérez E. Vanilla: Post-harvest Operations [Internet]. Lewis B, editor.
867 Rome, Italy: Food and Agriculture Organization of the United Nations (FAO); 2002.
868 https://openknowledge.fao.org/items/37cf7204-a9de-4c7a-8809-e259a22c298f

869 33. Marschner H. Marschner’s mineral nutrition of higher plants. 3rd edn. London:
870 Academic press; 2012. https://doi.org/10.1016/C2009-0-63043-9

871 34. International Organization for Standardization. Water quality — Determination
872 of selected elements by inductively coupled plasma optical emission
873 spectrometry (ICP-OES) (ISO 11885:2007); English version EN ISO 11885:2009
874 [Internet]. Brussels: European Committee for Standardization (CEN); 2009 June.

875 35. Knauf Performance Materials GmbH. PERLIGRAN® technical data sheet
876 [Internet]. Dortmund, Germany: Knauf Performance Materials GmbH; 2023.
877 https://knauf.com/api/download-center/v1/assets/9e042881-0fb1-431b-a3e1-
878 c45034586a98?download=true

879 36. Schindelin J, Arganda-Carreras I, Frise E, Kaynig V, Longair M, Pietzsch T, et
880 al. Fiji: an open-source platform for biological-image analysis. Nat Methods.
881 2012;9(7):676–82. https://doi.org/10.1038/nmeth.2019

882 37. European Commission. Commission Regulation (EC) No 152/2009 of 27
883 January 2009 laying down the methods of sampling and analysis for the official

884 control of feed [Internet]. Luxembourg: Publications Office of the European Union;
885 2009 Feb pp. 1–130. Report No.: CELEX:32009R0152.

886 38. Deutsches Institut für Normung, International Organization for
887 Standardization. DIN EN ISO 16634-1:2009-07 - Food products - Determination of
888 the total nitrogen content by combustion according to the Dumas principle and
889 calculation of the crude protein content - Part 1: Oilseeds and animal feeding
890 stuffs (ISO 16634-1:2008); German version EN ISO 16634-1:2008 [Internet].
891 Berlin: Beuth Verlag; 2009 July. Report No.: DIN EN ISO 16634-1:2009-07.

892 39. Deutsches Institut für Normung, International Organization for
893 Standardization. DIN EN ISO 17294-2:2024-12 - Water quality - Application of
894 inductively coupled plasma mass spectrometry (ICP-MS) - Part 2: Determination
895 of selected elements including uranium isotopes (ISO 17294-2:2023, Corrected
896 version 2024-02); German version EN ISO 17294-2:2023 [Internet]. Berlin: Beuth
897 Verlag; 2024 Dec. Report No.: DIN EN ISO 17294-2:2024-12.

898 40. Deutsches Institut für Normung, European Committee for Standardization.
899 DIN EN 13805:2014-12 - Foodstuffs - Determination of trace elements - Pressure
900 digestion; German version EN 13805:2014 [Internet]. Berlin: Beuth Verlag; 2014
901 Dec. Report No.: DIN EN 13805:2014-12.

902 41. Valladares F, Niinemets Ü. Shade Tolerance, a Key Plant Feature of Complex
903 Nature and Consequences. Annual Review of Ecology, Evolution, and
904 Systematics. 2008;39(Volume 39, 2008):237–57.
905 https://doi.org/10.1146/annurev.ecolsys.39.110707.173506

906 42. Martinez-Garcia JF, Rodriguez-Concepcion M. Molecular mechanisms of shade
907 tolerance in plants. New Phytologist. 2023;239(4):1190–202.
908 https://doi.org/10.1111/nph.19047

909 43. Euring D, Bai H, Janz D, Polle A. Nitrogen-driven stem elongation in poplar is
910 linked with wood modification and gene clusters for stress, photosynthesis and
911 cell wall formation. BMC Plant Biol. 2014;14(1):391.
912 https://doi.org/10.1186/s12870-014-0391-3

913 44. Maxwell K, Johnson GN. Chlorophyll fluorescence—a practical guide. J Exp Bot.
914 2000;51(345):659–68. https://doi.org/10.1093/jexbot/51.345.659

915 45. Ritchie GA. Chlorophyll fluorescence: What is it and what do the numbers
916 mean? In: Riley, LE; Dumroese, RK; Landis, TD, tech coords 2006 National
917 Proceedings: Forest and Conservation Nursery Associations - 2005 Proc RMRS-P-
918 43 Fort Collins, CO: US Department of Agriculture, Forest Service, Rocky
919 Mountain Research Station p 34-42. 2006;043.

920 46. Ruban AV. Nonphotochemical Chlorophyll Fluorescence Quenching:
921 Mechanism and Effectiveness in Protecting Plants from Photodamage. Plant
922 Physiol. 2016;170(4):1903–16. https://doi.org/10.1104/pp.15.01935

923 47. Ko S-S, Jhong C-M, Lin Y-J, Wei C-Y, Lee J-Y, Shih M-C. Blue Light Mediates
924 Chloroplast Avoidance and Enhances Photoprotection of Vanilla Orchid. IJMS.
925 2020;21(21):8022. https://doi.org/10.3390/ijms21218022

926 48. Hitsuda K, Yamada M, Klepker D. Sulfur Requirement of Eight Crops at Early
927 Stages of Growth. Agronomy Journal. 2005;97(1):155–9.
928 https://doi.org/10.2134/agronj2005.0155a

49. Mao Y, Chai X, Zhong M, Zhang L, Zhao P, Kang Y, et al. Effects of nitrogen and magnesium nutrient on the plant growth, quality, photosynthetic characteristics, antioxidant metabolism, and endogenous hormone of Chinese kale (*Brassica albograbra* Bailey). Scientia Horticulturae. 2022;303:111243. https://doi.org/10.1016/j.scienta.2022.111243

50. Eaton FM. Toxicity and accumulation of chloride and sulfate salts in plants. Journal of Agricultural Research. 1942;64:357-399.

51. Qu S, Li H, Zhang X, Gao J, Ma R, Ma L, et al. Effects of Magnesium Imbalance on Root Growth and Nutrient Absorption in Different Genotypes of Vegetable Crops. Plants. 2023;12(20):3518. https://doi.org/10.3390/plants12203518

52. Zotz G, Hietz P. The physiological ecology of vascular epiphytes: current knowledge, open questions. J Exp Bot. 2001;52(364):2067–78. https://doi.org/10.1093/jexbot/52.364.2067

53. Hikosaka K. Interspecific difference in the photosynthesis–nitrogen relationship: patterns, physiological causes, and ecological importance. J Plant Res. 2004;117(6):481–94. https://doi.org/10.1007/s10265-004-0174-2

54. Zotz G, Winter K. Annual carbon balance and nitrogen-use efficiency in tropical C3 and CAM epiphytes. New Phytologist. 1994;126(3):481–92. https://doi.org/10.1111/j.1469-8137.1994.tb04245.x

55. Markwell J, Osterman JC, Mitchell JL. Calibration of the Minolta SPAD-502 leaf chlorophyll meter. Photosynth Res. 1995;46(3):467–72. https://doi.org/10.1007/BF00032301

56. Marenco RA, Antezana-Vera SA, Nascimento HCS. Relationship between specific leaf area, leaf thickness, leaf water content and SPAD-502 readings in six Amazonian tree species. Photosynthetica. 2009;47(2):184–90. https://doi.org/10.1007/s11099-009-0031-6